

# Harnessing cloud computing for high capacity analysis of neuroimaging data from NDAR



Daniel Clark<sup>1</sup>, Christian Haselgrove<sup>2</sup>, David Kennedy<sup>2</sup>, Zhizhong Liu<sup>3</sup>,  
Michael Milham<sup>1</sup>, Petros Petrosyan<sup>4</sup>, Carinna Torgerson<sup>3</sup>, John Van Horn<sup>3</sup>, Cameron Craddock<sup>1</sup>

<sup>1</sup>Child Mind Institute, New York, NY, <sup>2</sup> University of Massachussetts Medical School, Worcester, MA, <sup>3</sup>University of Souther California, Los Angeles, CA, <sup>4</sup>UCLA, Los Angeles, CA, <sup>5</sup>Nathan S. Kline Institute for Psychiatric Research, Orangeburg, NY

## Introduction

- ▶ The default network (DN) is consistently deactivated relative to cognitive tasks in healthy controls, leading to the hypothesis that DN interference with task positive networks can lead to psychiatric disorders such as depression, autism, and anxiety<sup>1-7</sup>.
- ▶ Direct evaluation of DN dysregulation is challenging and is often inferred from reduced deactivation during task performance.
- ▶ Emerging real-time fMRI (rtfMRI) neurofeedback techniques have the potential to probe this phenomenon with more specificity<sup>8,9</sup>.

## Methods

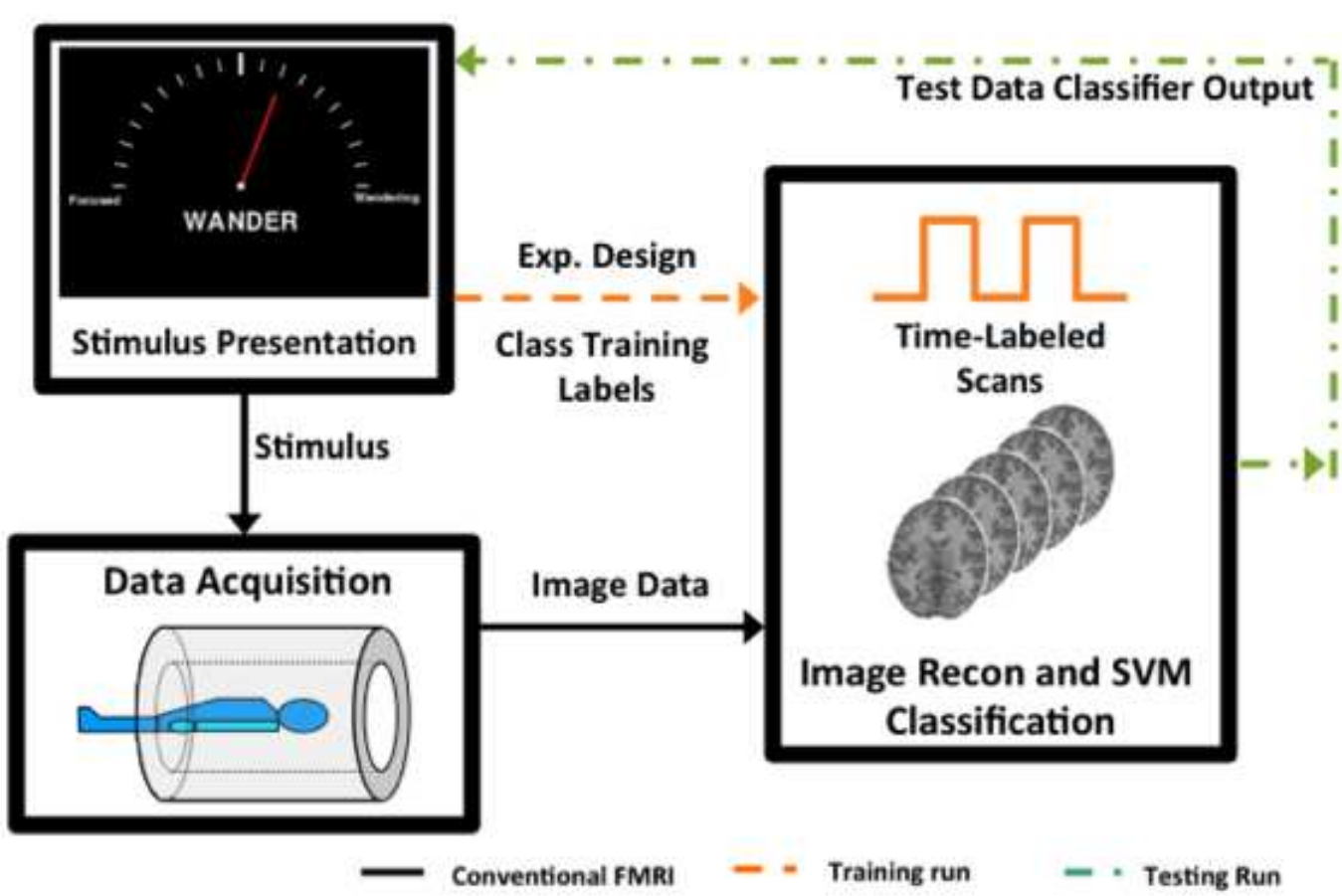


Figure 1 : Neurofeedback experiment, adapted from S. LaConte<sup>8,9</sup>

### Online Preprocessing

- ▶ RT denoising implemented in AFNI<sup>10</sup> to remove contributions of confounds (intensity modulations induced by head motion, physiological noise, scanner drift, ...)
  - ▶  $N^{th}$  order polynomial
  - ▶ Global mean
  - ▶ Mask average time series (i.e. WM, CSF)
  - ▶ Motion parameters (6 or 24 regressor models)
  - ▶ Spatial smoothing
- ▶ Adds < 5 ms of delay

### Subjects

- ▶ 13 volunteers participated in accordance with IRB Policy.

### Scanning

- ▶ 3.0T Siemens Magnetom TIM Trio using 12-channel head matrix.
  - ▶ T1 weighted 3D MPRAGE anatomical scan (FA=8°, TI=900ms, TR=2600ms, TE=3.02ms, GRAPPA ×2)
  - ▶ Realtime fMRI experiments were performed using an EPI sequence that has been customised to export reconstructed image volumes, over a network connection, as they are connected<sup>8,9</sup>
    - ▶ TR/TE/FA/FOV = 2000 ms/30 ms/90°/220 mm, in plane resolution  $3.44 \times 3.44 \times 4 \text{ mm}^3$

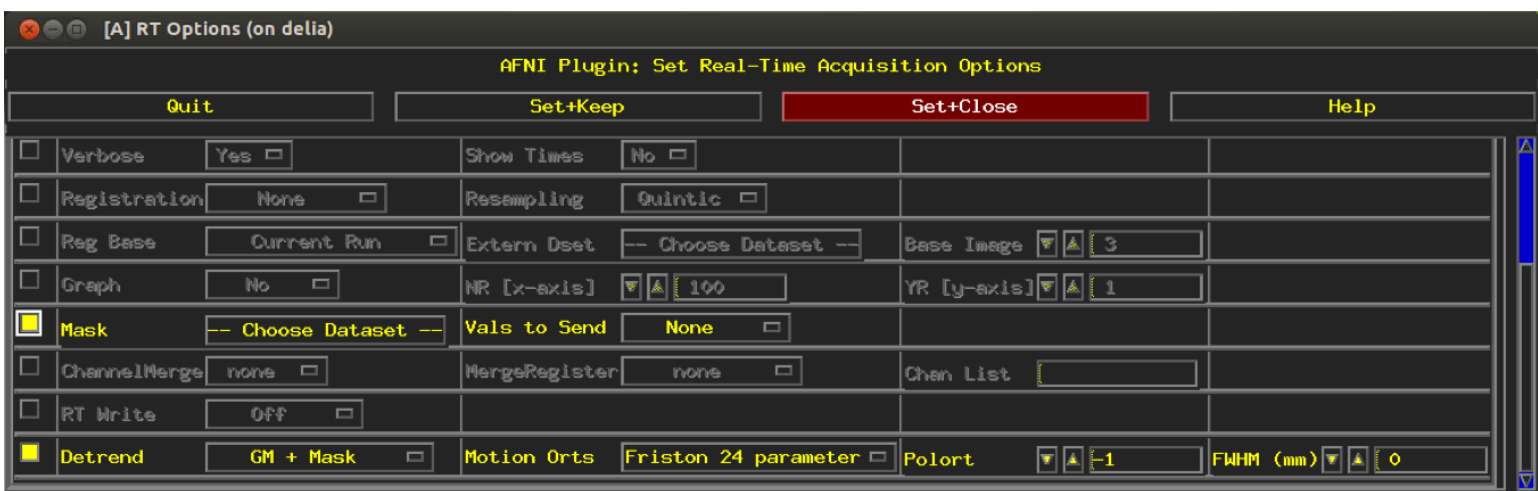


Figure 2 : AFNI interface for online denoising.

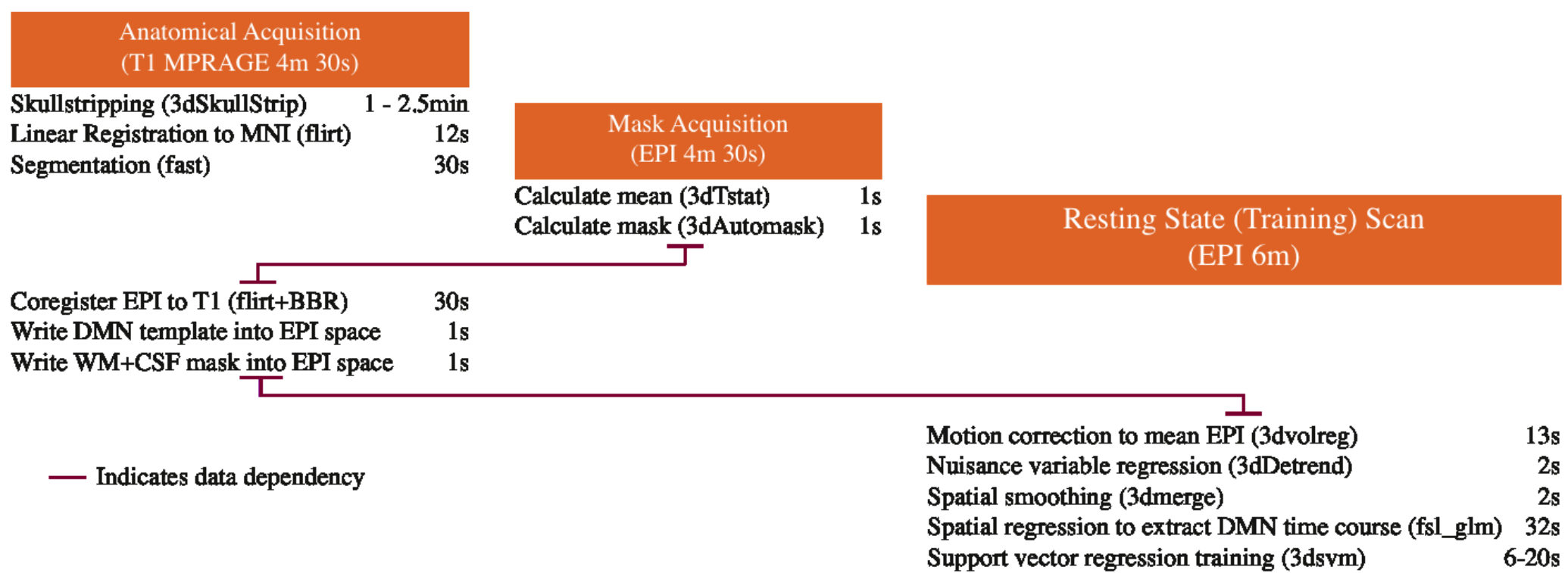


Figure 3 : Flow chart of neurofeedback experiment.

## Results

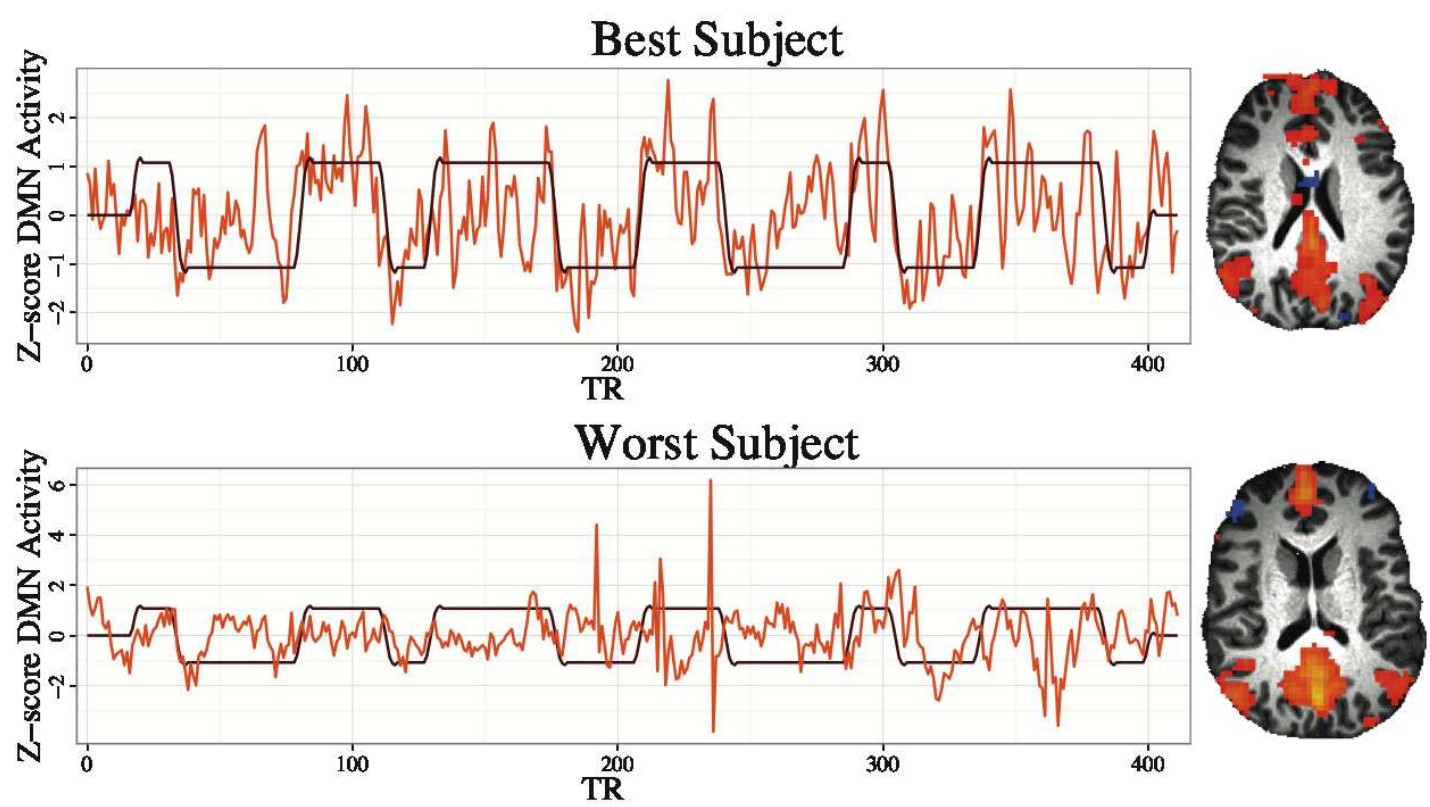


Figure 4 : Example of classifier and feedback timecourse for participants with the best and worst performance.

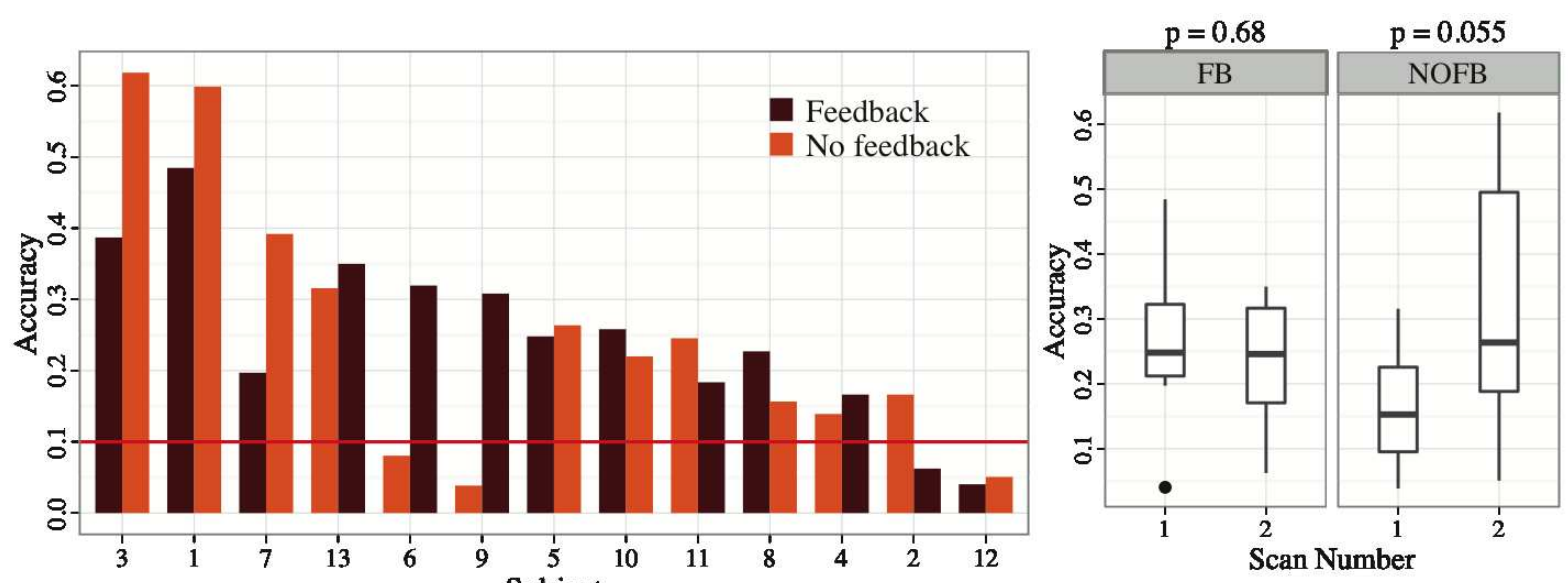


Figure 5 : Performance across participants (A) differs between feedback and neurofeedback scans as determined by their order (B).

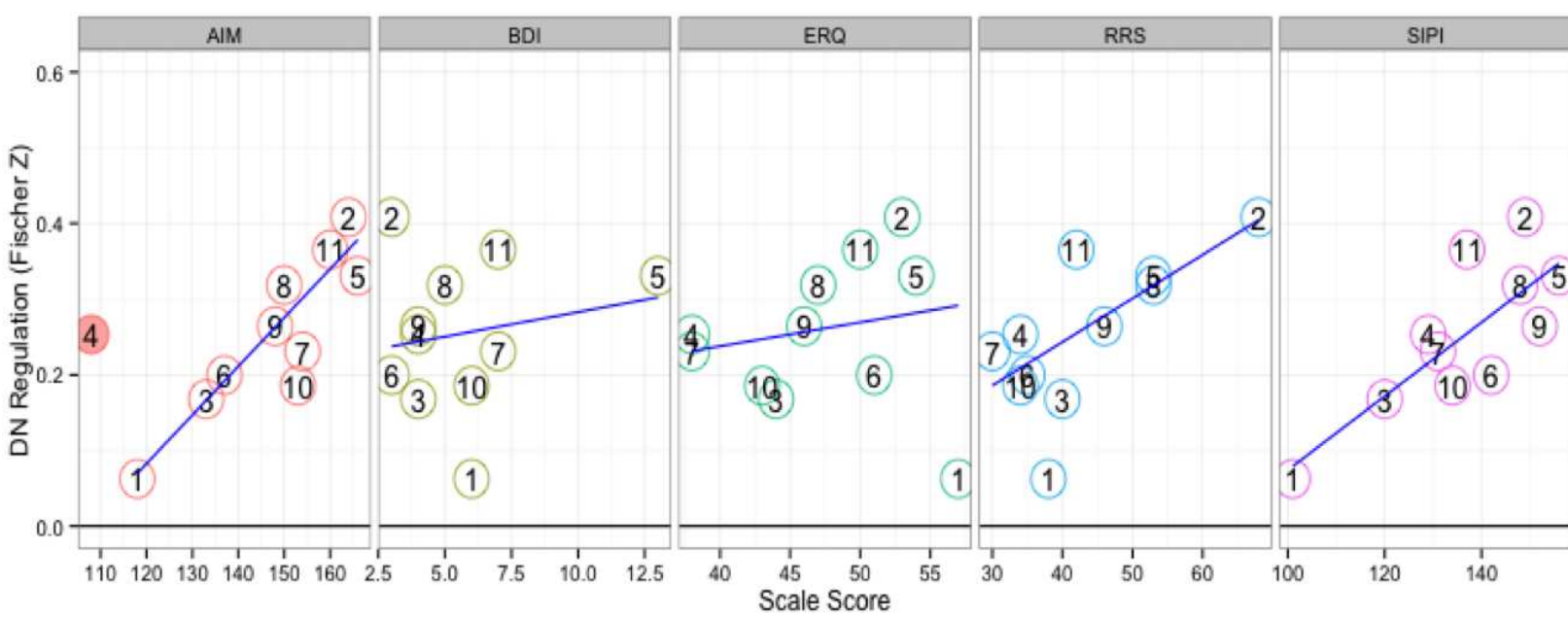


Figure 6 : Inter-individual variation in performance correlates with behavioral measures.

- ▶ As shown in figure 4 models learned for the best and worst performing participants match with the canonical pattern of the default network.
- ▶ The best participant was able to follow the instructions very well 4, the worst seems to have been corrupted by noise.
- ▶ Figure 5 shows 12 of the subjects were able to modulate the DN at above chance levels, performance on feedback runs is consistent independent of order, but performance on nonfeedback runs improves if they occur after feedback runs.
- ▶ Measures that were significantly associated with DN regulation include ( $p < 0.05$ , FDR corrected): the affect intensity measure (AIM), ruminative responses scale (RRS), and the imaginal processes inventory.

## Conclusion

- ▶ We developed a system for measuring DN regulation using realtime neurofeedback.
- ▶ Participants were able to modulate their DN activity and their ability to do so was correlated with phenotype.
- ▶ This system provides a new experimental paradigm for understanding network dysregulation and how it maps to disease states and phenotype.

## References and Acknowledgements

1. Sonuga-Barke, E. et al. (2007), Neuroscience and Biobehavioral Reviews 31:977-986.
2. Broyd, S. J. et al. (2009), Neuroscience and Biobehavioral Reviews 33: 279-296.
3. Sheline, Y.I. et al. (2009), PNAS 106: 1942-1947.
4. Whitfield-Gabrieli, S. et al. (2009), PNAS 106: 1279-1284.
5. Hamilton, J.P. et al. (2011), Biol. Psychiatry 70: 327-333.
6. Sylvester, C.M. et al. (2012), Trends Neurosci. 35, 527-535.
7. Castellanos, F.X. et al. (2012), Trends Cogn. Sci. 16, 17-26.
8. LaConte, S.M. et al. (2004). Human Brain Mapping, 11: 2551.
9. LaConte, S.M. et al. (2011). NeuroImage, 56(2), 440-454.
10. Cox, R.W. (1996) Comput. Biomed. Res. 29: 162-173.

Data collection and salary support was provided by a NARSAD Young Investigator Award to RCC.